Acta Crystallographica Section C
Crystal Structure Communications
ISSN 0108-2701

2-(2-Acetylamino-5-chlorophenyl)-2,2-difluoroethanoic acid and 2-(2-acetylamino-5-methylphenyl)-2,2-difluoroethanoic acid, and 2-(2-acetylaminophenyl)-2,2-difluoro-*N*-phenylacetamide and 2-(2-acetylaminophenyl)-*N*-(4-chlorophenyl)-2,2-difluoroacetamide: examples of variation in molecular packing and hydrogen-bonding motif induced by substituent change

Nubia Boechat,[a] Lindalva C. Maciel,[a] Angelo C. Pinto,[b] Solange M. S. V. Wardell,[a] Janet M. S. Skakle[c] and R. Alan Howie[c]*

[a]Fundaçâo Oswaldo Cruz, Far-Manguinhos, Rua Sizenando Nabuco 100, Manguinhos, 21041250 Rio de Janeiro, RJ, Brazil, [b]Instituto de Química, Departamento de Química Orgânica, Universidade Federal de Rio de Janeiro, Ilha do Fundão, Rio de Janeiro, CEP 21941-590, Brazil, and [c]Department of Chemistry, University of Aberdeen, Meston Walk, Aberdeen AB24 3UE, Scotland
Correspondence e-mail: r.a.howie@abdn.ac.uk

Received 24 January 2005
Accepted 9 March 2005
Online 2 April 2005

Among the title compounds, *viz*. the acids $C_{10}H_8ClF_2NO_3$, (I), and $C_{11}H_{11}F_2NO_3$, (II), and the amides $C_{14}H_{14}F_2N_2O_2$, (III), and $C_{14}H_{13}ClF_2N_2O_2$, (IV), the change of substituent from Cl in (I) to methyl in (II) has a dramatic effect upon the hydrogen bonding between the molecules, which occur in layers in both cases. In the structures of (III) and (IV), hydrogen bonds connect the molecules to form chains, but the introduction of a chloro substituent in (IV) has a profound effect on the orientation of the molecules within the chains and the packing of the chains in the structure as a whole.

Comment

Boechat & Pinto (2000) have investigated the syntheses and pharmaceutical potential of a series of difluorinated ethanoic acids and their amide derivatives. Such compounds were obtained by the nucleophilic cleavage, using water or amines, of 3,3-difluoroindol-2-ones prepared from appropriately substituted indoline-2,3-diones (isatins) and (diethylamino)sulfur trifluoride. Presented here are the crystal structures and supramolecular arrangements of the title four representative compounds, (I)–(IV) (see scheme).

The molecules of (I) to (IV) are shown in Figs. 1–4. With the exception of the numbering of the F atoms and the cyclic order of the benzene ring defined by atoms C11–C16 in the amides (R_2 as opposed to R_1 for the ring defined by atoms C1–C6), all four molecules are labelled in the same manner. This makes possible the gathering together of selected bond lengths and angles for all four compounds, as shown in Table 1. The

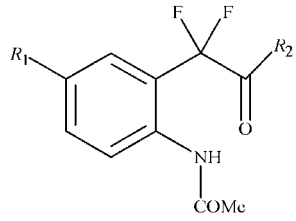

(I) R_1=Cl; R_2=OH
(II) R_1=Me; R_2=OH
(III) R_1=H; R_2=NHPh
(IV) R_1=H; R_2=NH-C_6H_4-*p*-Cl

distances and angles within the benzene rings, in the ranges 1.359 (5)–1.410 (5) Å and 118.0 (2)–121.9 (4)°, respectively, are generally as expected. It is noticeable, however, that the spread of distances is greater in the R_1 rings, especially in the case of (I), than it is in the R_2 rings of the amides. The same is true, but to a lesser degree, for the angles. Of particular interest in Table 1 are the torsion angles around the C7—C8 and C2—N1 bonds, which are very diffent for (I) compared with the other compounds. Also notable in the case of (I) is the large displacement [0.210 (7) Å] of atom C7 from the least-squares plane of ring R_1. The next largest displacement of an atom directly attached to a benzene ring [0.115 (3) Å] is

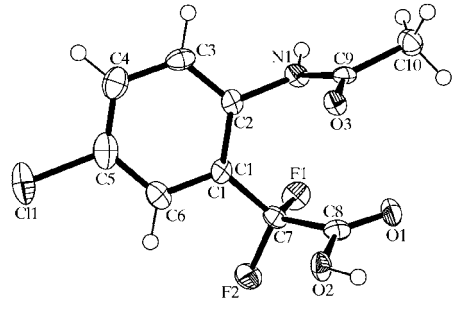

Figure 1
A view of (I), showing the atom-numbering scheme. Displacement ellipsoids are drawn at the 50% probability level and H atoms are shown as small spheres of arbitrary radii.

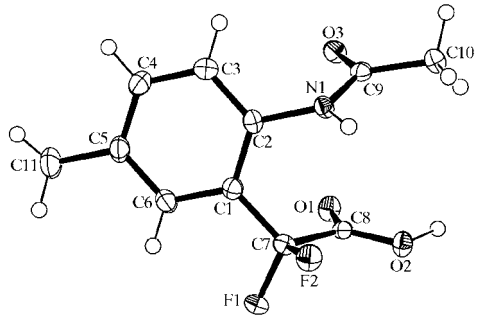

Figure 2
A view of (II), showing the atom-numbering scheme. Displacement ellipsoids are drawn at the 50% probability level and H atoms are shown as small spheres of arbitrary radii.

  DOI: 10.1107/S0108270105007547

that of atom N2 relative to ring R_2 of (IV). In both of these, the displaced atoms are *para* to a Cl ring substituent. In the amides, the dihedral angles between the rings R_1 and R_2, as defined above, are 75.06 (6) and 82.27 (6)° for (III) and (IV), respectively.

In all four structures, hydrogen bonds (Tables 2–5) play a major part in controlling the supramolecular assembly of the molecules. In the structure of (I), the O2—H2···O3 and N1—H1···O3 hydrogen bonds (Table 2) have completely different roles. The O2—H2···O3 hydrogen bonds create dimers (Fig. 5) with motif $R_2^2(18)$, according to the notation of Bernstein *et al.* (1995). The N1—H1···O3 hydrogen bonds then create larger $R_6^4(26)$ rings (Fig. 6). Overall, the molecules are found interconnected in layers parallel to (001) (Fig. 7), in which the hexameric $R_6^4(26)$ rings provide cavities within which are found the F atoms and oxo atom O1 of the carboxylate group, which play no part in hydrogen-bond formation. As shown in Fig. 7, the larger hexameric rings are connected in a herring-bone fashion to complete the layer. The layers, with Cl atoms on their surfaces, are then stacked in the *a* direction and are related to one another purely by cell translation. There are no interactions between the layers other than van der Waals contacts; this explains the occurrence of the stacking faults, which necessitated the twin refinement of this structure, as described below.

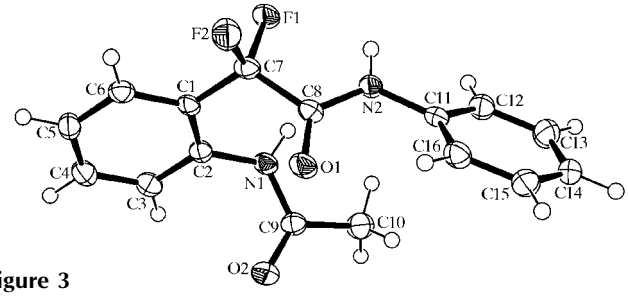

Figure 3
A view of (III), showing the atom-numbering scheme. Displacement ellipsoids are drawn at the 50% probability level and H atoms are shown as small spheres of arbitrary radii.

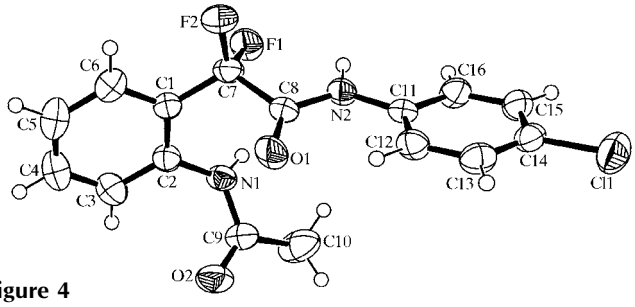

Figure 4
A view of (IV), showing the atom-numbering scheme. Displacement ellipsoids are drawn at the 50% probability level and H atoms are shown as small spheres of arbitrary radii.

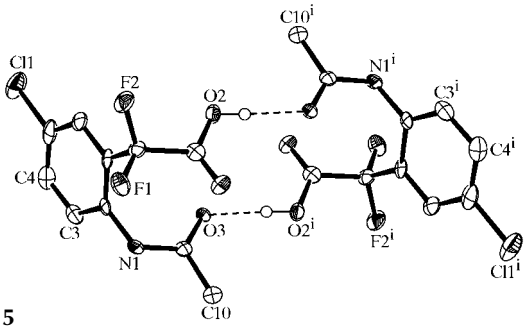

Figure 5
The centrosymmetric $R_2^2(18)$ motif in (I). Displacement ellipsoids are drawn at the 50% probability level and H atoms involved in hydrogen bonds (dashed lines) are shown as small spheres of arbitrary radii. Selected atoms are labelled. For the sake of clarity, the unit-cell outline has been omitted. [Symmetry code: (i) $1-x, 1-y, 1-z$.]

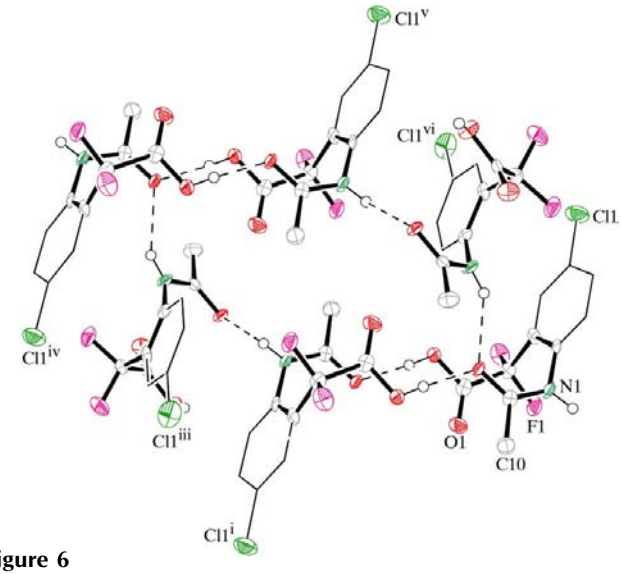

Figure 6
The hexamolecular $R_6^4(26)$ motif in (I). For clarity, bonds to atoms C3–C6 are shown as thin lines. Displacement ellipsoids are drawn at the 50% probability level and H atoms involved in hydrogen bonds (dashed lines) are shown as small spheres of arbitrary radii. Selected atoms are labelled, primarily to provide a key for the coding of the ellipsoids, which is the same for all of Figs. 6–9, 11 and 13. For the sake of clarity, the unit-cell outline has been omitted. [Symmetry codes: (i) $1-x, 1-y, 1-z$; (iii) $1-x, \frac{1}{2}+y, \frac{3}{2}-z$; (iv) $1-x, 1-y, 2-z$; (v) $x, y, 1+z$; (vi) $x, \frac{1}{2}-y, \frac{1}{2}+z$.]

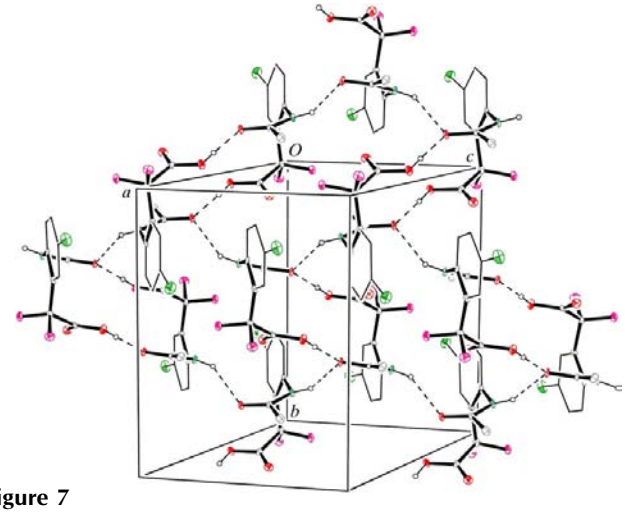

Figure 7
A more extensive view of the hydrogen-bonding within a layer of molecules of (I). The representation is the same as in Fig. 6, except that the displacement ellipsoids are now at the 20% probability level, symmetry codes and atom labels have been omitted and the outline of the unit cell is shown.

In (II), O2—H2···O3 hydrogen bonds (Table 3) connect the molecules, with each molecule related to its neighbour by the operation of a crystallographic twofold screw axis, forming zigzag chains propagated in the *b* direction. N1—H1···O1 hydrogen bonds connect the chains, related to one another by cell translation, in the *a* direction. This creates the $R_4^4(24)$ motif shown in Fig. 8. Replication of this motif results in the formation of layers of molecules parallel to (001), as shown in Fig. 9. The surfaces of the layers are populated by methyl groups (atom C11 and the H atoms attached to it) and only van der Waals interactions occur at the layer interface.

N—H···O hydrogen bonds in (III) (Table 4) connect molecules, related to one another by cell translation, to form chains propagated in the *a* direction, as shown in Fig. 10. The contribution of each of the N—H···O hydrogen bonds to the connectivity of the chain is a four-atom repeat unit, *e.g.* N1, H1, $O2^{i}$ and $C9^{i}$ [symmetry code: (i) $x-1, y, z$] for the first of the hydrogen bonds given in Table 4. Taken together in pairs, the hydrogen bonds create rings which recur along the length of the chain. The overall connectivity can then be represented by the graph set $C(4)R_2^2(16)$. The distribution of the chains in the unit cell, and hence in the complete structure, where they are related to one another by crystallographic centres of symmetry, is shown in Fig. 11, where the chains are seen end-on. Only van der Waals interactions occur between neighbouring chains.

In (IV), as in (III), N—H···O hydrogen bonds (Table 5) connect the molecules to form chains. However, the chains

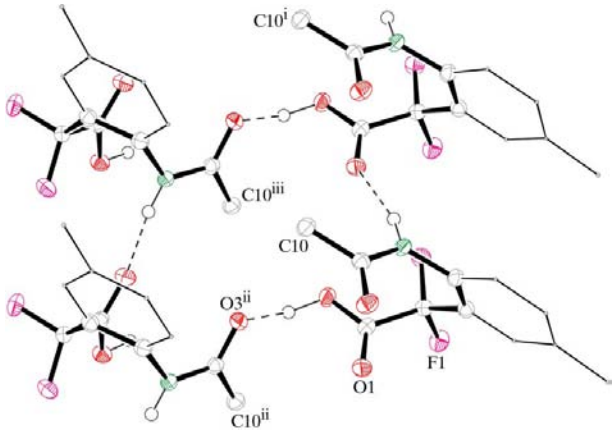

Figure 8
The $R_4^4(24)$ motif in (II). For clarity, bonds to atoms C3–C6 and C11 are shown as thin lines. Ellipsoids are drawn at the 50% probability level and H atoms involved in hydrogen bonds (dashed lines) are shown as small spheres of arbitrary radii. Coding is indicated by the labelling of selected atoms. For the sake of clarity, the unit-cell outline has been omitted. [Symmetry codes: (i) $x-1, y, z$; (ii) $1-x, \frac{1}{2}+y, 1-z$; (iii) $x, \frac{1}{2}+y, 1-z$.]

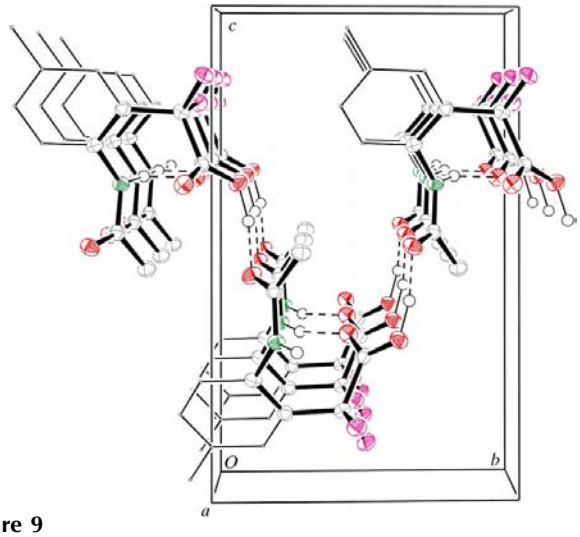

Figure 9
A more extensive view of the hydrogen bonding within a layer of molecules of (II). The representation is the same as in Fig. 8, except that the outline of the unit cell is shown, while atom labels and symmetry codes have been omitted.

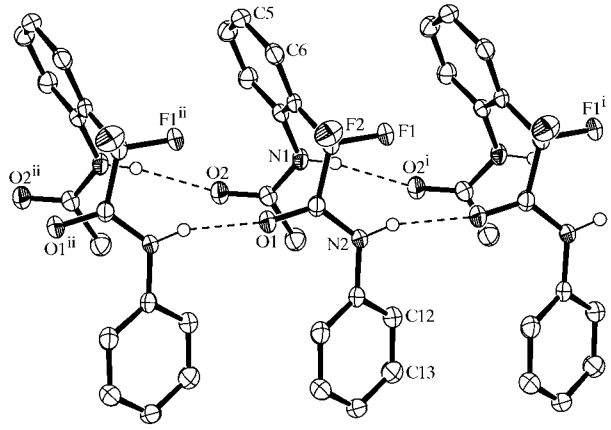

Figure 10
A hydrogen-bonded chain in (III). Displacement ellipsoids are drawn at the 50% probability level and H atoms involved in hydrogen bonds (dashed lines) are shown as small spheres of arbitrary radii. Selected atoms are labelled. For the sake of clarity, the unit-cell outline has been omitted. [Symmetry codes: (i) $x-1, y, z$; (ii) $x+1, y, z$.]

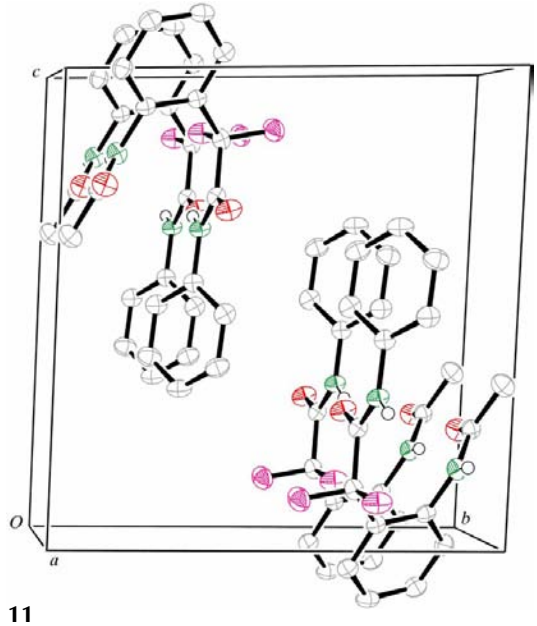

Figure 11
The packing of the hydrogen-bonded chains of molecules in (III). Displacement ellipsoids are drawn at the 50% probability level and H atoms involved in hydrogen bonds are shown as small spheres of arbitrary radii. The coding of the atoms is the same as in Figs. 6–9.

(Fig. 12) are now propagated in the *c* direction and adjacent molecules are related by the operation of a crystallographic *c*-glide plane. Despite the molecules now alternating in orientation along the length of the chain, the $C(4)R_2^2(16)$ graph set assigned to the situation in (III) also applies to (IV). The chains in (IV) are distributed in such a way as to bring about face-to-face π–π contacts between pairs of centrosymmetrically related benzene rings (R_2) of the *N*-phenyl groups. These are shown in Fig. 13 distributed in an A-face-centred arrangement. For this interaction, in which the centrosymmetric relationship (symmetry code: $-x$, $1-y$, $1-z$) renders the least-squares planes of the overlapping rings parallel, the distance between the ring centroids, the perpendicular distance between their least-squares planes and the lateral displacement or slippage of the rings are 3.803, 3.473 and 1.550 Å, respectively. The combination of the hydrogen bonding within the chains and pairwise overlap of the phenyl groups interconnects the molecules to form layers parallel to (100). The Cl atoms are confined to a region at the centre of the layer, while the layer surfaces are occupied by the methyl groups (atom C10 and the attached H atoms) of the acetamide group and by the atoms of the C3—C4 edge of the ring defined by atoms C1–C6 (R_1).

The difference in structure between acids (I) and (II) must be due to the difference in the substituents at the 5-position of the benzene ring, *viz*. Cl for (I) and Me for (II). The essential difference between the two structures, *i.e.* the non-participation in hydrogen bonding of atom O1 in (I), suggests that electronic effects arising from the electronegativity and the position of Cl on the ring have brought this about. The structural differences between acids (I) and (II), on the one hand, and amides (III) and (IV) on the other, where, for the amides, utilization of all available hydrogen-bond donors and acceptors only creates chains of molecules rather than layers or sheets, is considered to be due to the need to accommodate the steric requirements of the *N*-phenyl groups of the amides. The difference between the structures of amides (III) and (IV), specifically in the manner in which the hydrogen-bonded chains of molecules are associated in pairs, is attributed to the presence of the Cl substituent in (IV), but is perceived as steric rather than electronic in origin.

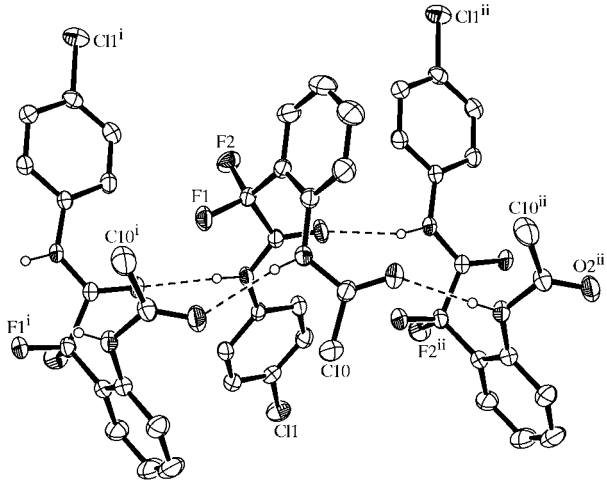

Figure 12
A hydrogen-bonded chain in (IV). Displacement ellipsoids are drawn at the 30% probability level and H atoms involved in hydrogen bonds (dashed lines) are shown as small spheres of arbitrary radii. Selected atoms are labelled. For the sake of clarity, the unit-cell outline has been omitted. [Symmetry codes: (i) $x, \frac{3}{2}-y, \frac{1}{2}+z$; (ii) $x, \frac{3}{2}-y, z-\frac{1}{2}$.]

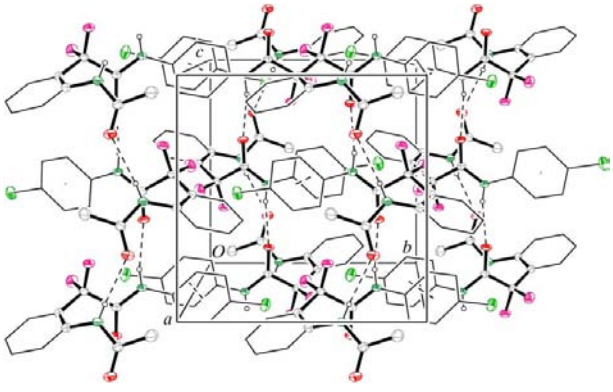

Figure 13
Intermolecular contacts within a layer of molecules of (IV). Displacement ellipsoids are drawn at the 20% probability level. For convenience, the origin of the cell has been shifted to $(-\frac{1}{2}, 0, 0)$. Dashed lines indicate the join of the centroids of overlapping benzene rings (see *Comment*) as well as hydrogen bonds. For clarity, bonds to atoms C3–C6 and C11–C16 are shown as thin lines. Coding is the same as for Figs. 6–9 and 11.

Experimental

Compounds (I)–(IV) were prepared by general procedures (Boechat & Pinto, 2000). Compound (I) (m.p. 438–440 K) was recrystallized from dichloroethane, (II) (m.p. 437–440 K) from MeOH, and both (III) (m.p. 441–443 K) and (IV) (m.p. 445–446 K) from EtOH.

Compound (I)

Crystal data

$C_{10}H_8ClF_2NO_3$
$M_r = 263.62$
Monoclinic, $P2_1/c$
$a = 11.5493$ (6) Å
$b = 11.6207$ (6) Å
$c = 8.5251$ (4) Å
$\beta = 107.334$ (2)°
$V = 1092.20$ (10) Å^3
$Z = 4$
$D_x = 1.603$ Mg m^{-3}
Mo $K\alpha$ radiation
Cell parameters from 2529 reflections
$\theta = 2.9$–$27.5°$
$\mu = 0.37$ mm^{-1}
$T = 120$ (2) K
Plate, colourless
0.60 × 0.25 × 0.05 mm

Data collection

Bruker–Nonius KappaCCD area-detector diffractometer
φ and ω scans
13 369 measured reflections
13 369 independent reflections
6202 reflections with $I > 2\sigma(I)$
$R_{int} = 0.000$
$\theta_{max} = 27.5°$
$h = -14 \rightarrow 14$
$k = -15 \rightarrow 15$
$l = -10 \rightarrow 10$

Refinement

Refinement on F^2
$R[F^2 > 2\sigma(F^2)] = 0.121$
$wR(F^2) = 0.330$
$S = 1.57$
13 369 reflections
160 parameters
H atoms treated by a mixture of independent and constrained refinement
$w = 1/[\sigma^2(F_o^2) + (0.1P)^2]$ where $P = (F_o^2 + 2F_c^2)/3$
$(\Delta/\sigma)_{max} < 0.001$
$\Delta\rho_{max} = 1.28$ e Å^{-3}
$\Delta\rho_{min} = -0.72$ e Å^{-3}

Table 1
Selected geometric parameters (Å, °) for compounds (I)–(IV).

	(I)†	(II)‡	(III)§	(IV)§
C2—N1	1.433 (5)	1.435 (3)	1.426 (3)	1.419 (2)
C5—*X*	1.753 (4)	1.507 (3)		
C8—O1	1.202 (5)	1.213 (3)	1.229 (2)	1.2158 (19)
C8—O2	1.330 (4)	1.298 (3)	1.340 (3)	1.333 (2)
C9—N1	1.333 (5)	1.346 (3)	1.366 (3)	1.352 (2)
C9—O3	1.250 (4)	1.242 (3)	1.228 (2)	1.222 (2)
C9—C10	1.512 (5)	1.495 (3)	1.492 (3)	1.490 (3)
C11—N2			1.418 (3)	1.420 (2)
C14—Cl1				1.7424 (19)
C1—C7—C8	119.5 (4)	112.92 (18)	116.77 (18)	115.46 (14)
O1—C8—O2	127.1 (4)	126.2 (2)	125.5 (2)	126.13 (16)
O1—C8—C7	123.1 (4)	118.7 (2)	118.69 (19)	117.85 (15)
O2—C8—C7	109.7 (4)	115.0 (2)	115.77 (18)	115.85 (14)
C8—N2—C11			125.84 (18)	127.67 (14)
C9—N1—C2	120.9 (4)	121.82 (19)	122.86 (17)	123.54 (16)
O3—C9—N1	121.2 (4)	120.6 (2)	122.2 (2)	122.77 (19)
O3—C9—C10	121.8 (4)	121.67 (19)	122.7 (2)	122.22 (19)
N1—C9—C10	116.9 (4)	117.7 (2)	115.10 (19)	115.01 (18)
C1—C7—C8—O1	−113.6 (5)	−44.0 (3)	−49.4 (3)	−33.8 (2)
C1—C7—C8—O2	68.2 (5)	136.4 (2)	131.7 (2)	150.49 (15)
C3—C2—N1—C9	103.1 (5)	−64.3 (3)	−59.0 (3)	−51.4 (3)
C1—C2—N1—C9	−76.7 (5)	112.8 (2)	120.4 (2)	128.08 (19)

† *X* = Cl1. ‡ *X* = methyl C11. § For O2 read N2 and for O3 read O2.

Table 2
Hydrogen-bond geometry (Å, °) for (I).

D—H···*A*	*D*—H	H···*A*	*D*···*A*	*D*—H···*A*
O2—H2···O3^{i}	0.84	1.73	2.570 (4)	176
N1—H1···O3^{ii}	0.88 (4)	2.23 (4)	3.014 (4)	148 (3)

Symmetry codes: (i) $-x+1, -y+1, -z+1$; (ii) $x, -y+\frac{1}{2}, z-\frac{1}{2}$.

Compound (II)

Crystal data

$C_{11}H_{11}F_2NO_3$
M_r = 243.21
Monoclinic, $P2_1$
a = 4.9174 (3) Å
b = 8.3976 (3) Å
c = 13.5487 (7) Å
β = 91.208 (2)°
V = 559.36 (5) Å^3
Z = 2
D_x = 1.444 Mg m^{-3}
Mo $K\alpha$ radiation
Cell parameters from 1294 reflections
θ = 2.9–27.5°
μ = 0.13 mm^{-1}
T = 120 (2) K
Block, colourless
0.30 × 0.08 × 0.03 mm

Data collection

Bruker–Nonius KappaCCD area-detector diffractometer
φ and ω scans
Absorption correction: multi-scan (*SADABS*; Sheldrick, 2003)
T_{min} = 0.813, T_{max} = 1.000
5630 measured reflections
1373 independent reflections
1240 reflections with $I > 2\sigma(I)$
R_{int} = 0.032
θ_{max} = 27.5°
$h = -6 \rightarrow 6$
$k = -10 \rightarrow 10$
$l = -17 \rightarrow 17$

Refinement

Refinement on F^2
$R[F^2 > 2\sigma(F^2)]$ = 0.036
$wR(F^2)$ = 0.086
S = 1.08
1373 reflections
160 parameters
H atoms treated by a mixture of independent and constrained refinement
$w = 1/[\sigma^2(F_o^2) + (0.0465P)^2 + 0.1105P]$ where $P = (F_o^2 + 2F_c^2)/3$
$(\Delta/\sigma)_{max} < 0.001$
$\Delta\rho_{max}$ = 0.18 e Å^{-3}
$\Delta\rho_{min}$ = −0.23 e Å^{-3}

Table 3
Hydrogen-bond geometry (Å, °) for (II).

D—H···*A*	*D*—H	H···*A*	*D*···*A*	*D*—H···*A*
N1—H1···O1^{i}	0.94 (3)	1.97 (3)	2.884 (3)	165 (2)
O2—H2···O3^{ii}	0.84	1.67	2.502 (2)	169

Symmetry codes: (i) $x-1, y, z$; (ii) $-x+1, y+\frac{1}{2}, -z+1$.

Compound (III)

Crystal data

$C_{16}H_{14}F_2N_2O_2$
M_r = 304.29
Triclinic, $P\overline{1}$
a = 5.0075 (3) Å
b = 11.5863 (11) Å
c = 12.2219 (11) Å
α = 87.304 (4)°
β = 89.327 (5)°
γ = 78.588 (5)°
V = 694.30 (10) Å^3
Z = 2
D_x = 1.456 Mg m^{-3}
Mo $K\alpha$ radiation
Cell parameters from 6753 reflections
θ = 2.9–27.5°
μ = 0.12 mm^{-1}
T = 120 (2) K
Lath, colourless
0.20 × 0.13 × 0.08 mm

Data collection

Enraf–Nonius KappaCCD area-detector diffractometer
φ and ω scans
Absorption correction: multi-scan (*SORTAV*; Blessing, 1995, 1997)
T_{min} = 0.924, T_{max} = 1.000
5877 measured reflections
3177 independent reflections
1631 reflections with $I > 2\sigma(I)$
R_{int} = 0.071
θ_{max} = 27.6°
$h = -6 \rightarrow 6$
$k = -15 \rightarrow 14$
$l = -15 \rightarrow 15$

Refinement

Refinement on F^2
$R[F^2 > 2\sigma(F^2)]$ = 0.053
$wR(F^2)$ = 0.118
S = 0.94
3177 reflections
206 parameters
H atoms treated by independent and constrained refinement
$w = 1/[\sigma^2(F_o^2) + (0.0443P)^2]$ where $P = (F_o^2 + 2F_c^2)/3$
$(\Delta/\sigma)_{max} < 0.001$
$\Delta\rho_{max}$ = 0.26 e Å^{-3}
$\Delta\rho_{min}$ = −0.28 e Å^{-3}

Table 4
Hydrogen-bond geometry (Å, °) for (III).

D—H···*A*	*D*—H	H···*A*	*D*···*A*	*D*—H···*A*
N1—H1···O2^{i}	0.89 (2)	2.24 (2)	3.114 (2)	166 (2)
N2—H2···O1^{i}	0.87 (2)	2.06 (2)	2.875 (2)	156 (2)

Symmetry code: (i) $x-1, y, z$.

Table 5
Hydrogen-bond geometry (Å, °) for (IV).

D—H···*A*	*D*—H	H···*A*	*D*···*A*	*D*—H···*A*
N1—H1···O2^{i}	0.83 (2)	2.19 (2)	3.002 (2)	169 (2)
N2—H2···O1^{i}	0.84 (1)	2.07 (2)	2.8524 (18)	155 (2)

Symmetry code: (i) $x, -y+\frac{3}{2}, z+\frac{1}{2}$.

Compound (IV)

Crystal data

$C_{16}H_{13}ClF_2N_2O_2$
M_r = 338.73
Monoclinic, $P2_1/c$
a = 16.5777 (10) Å
b = 9.8176 (6) Å
c = 9.6962 (6) Å
β = 96.0100 (10)°
V = 1569.41 (17) Å^3
Z = 4
D_x = 1.434 Mg m^{-3}
Mo $K\alpha$ radiation
Cell parameters from 3620 reflections
θ = 2.4–31.2°
μ = 0.28 mm^{-1}
T = 291 (2) K
Block, colourless
0.48 × 0.23 × 0.17 mm

Data collection

Bruker SMART 1000 CCD area-detector diffractometer
φ and ω scans
Absorption correction: multi-scan (*SADABS*; Sheldrick, 2000)
T_{min} = 0.841, T_{max} = 1.000
15 368 measured reflections
5629 independent reflections
2824 reflections with $I > 2\sigma(I)$
R_{int} = 0.045
θ_{max} = 32.6°
$h = -20 \rightarrow 25$
$k = -14 \rightarrow 14$
$l = -14 \rightarrow 11$

Refinement

Refinement on F^2
$R[F^2 > 2\sigma(F^2)]$ = 0.055
$wR(F^2)$ = 0.132
S = 1.00
5629 reflections
215 parameters
H atoms treated by a mixture of independent and constrained refinement
$w = 1/[\sigma^2(F_o^2) + (0.0478P)^2 + 0.3392P]$ where $P = (F_o^2 + 2F_c^2)/3$
$(\Delta/\sigma)_{max} < 0.001$
$\Delta\rho_{max}$ = 0.26 e Å^{-3}
$\Delta\rho_{min}$ = −0.24 e Å^{-3}

The sample crystal of (I) was twinned, with major and minor twin components present, as indicated by the refinement, to the extent of 61.0 (1) and 39.0 (1)%, respectively. As a consequence, twin refinement by means of the *SHELXL97* HKLF 5 instruction (Sheldrick, 1997), which precludes merging of the data as part of the refinement process, was employed, along with intensity data containing a mixture of completely overlapping, partially overlapping and completely non-overlapping reflections identified as follows. For the cell corresponding to the space group $P2_1/a$ in use when the intensity data were collected, the COMPARECELL function of *DENZO* (Otwinowski & Minor, 1997) identified the presence of two reciprocal lattices relating to major and minor twin components, the reflections of which were assigned batch numbers 1 and 2, respectively. The two reciprocal lattices are related by rotation through 180° about **a***. The relationship between the Miller indices [$H(1)$, $K(1)$, $L(1)$ for the major component and $H(2)$, $K(2)$, $L(2)$ for the minor component], which is used to determine the presence or absence of points of coincidence of the two reciprocal lattices and therefore of overlap of reflections, is defined as $H(1) = H(2)$, $K(1) = -K(2)$, $L(1) = -[0.8 \times H(2) + L(2)]$. The criterion for overlap is the remainder, M, left after dividing $H(2)$ by 5; $M = 0$ implies complete overlap, and $M = 1$ or 4 implies partial but significant overlap [the calculated value of $L(1)$ will be non-integer by no more than $\pm \frac{1}{5}$]. In both of these cases, the measured intensity is shared between the code 2 reflection and the code 1 reflection with which it is paired. $M = 2$ or 3 indicates the total absence of overlap. The *.hkl* file used in the refinement contains, therefore, three groups of reflections, namely individual code 1 reflections associated exclusively with the major twin component, reflections in overlapping pairs with code −2 for the first and code 1 for the second, the intensity of which is to be shared between the two twin components and, finally, individual code 2 reflections associated exclusively with the minor twin component. The indices of the reflections in all of these groups were adjusted in the usual manner for the solution and refinement of the structure in the standard setting of the space group $P2_1/c$. The nature of the intensity data also precludes merging and multi-scan absorption correction as part of the data reduction process, and also creates difficulties in scaling the data. These difficulties combine to limit the refinement, yielding an R factor, in this case 0.121, rather higher than would be anticipated for a refinement of the usual kind. Also, on completion, this refinement revealed residual electron-density features of a peak of 1.28 e Å^{-3} 0.10 Å from atom Cl1 and a hole of −0.72 e Å^{-3} 1.47 Å from atom H10*C*.

In the absence of any element of atomic number higher than F, the refinement of the structure of (II) in the non-centrosymmetic space group $P2_1$ was carried out on merged intensity data. The Flack (1983) parameter is therefore indeterminate, so the absolute structure could not be determined.

In all four refinements, aryl and methyl H atoms were placed in calculated positions, with C—H distances of 0.95 and 0.98 Å, respectively, for (I)–(III), and 0.93 and 0.96 Å, respectively, for (IV), and refined with a riding model, with $U_{iso}(H) = 1.2U_{eq}(C)$ for aryl H atoms and $1.5U_{eq}(C)$ for methyl H atoms. The orientations of the methyl groups were also refined. The positions of the amide H atoms of (I), (II) and (IV), and of the hydroxyl H atoms of (I) and (II), were obtained from difference maps. The amide H atoms of (III) were initially placed in the manner of aryl H atoms. The coordinates of all amide H atoms of all four compounds were refined, with $U_{iso}(H) = 1.2U_{eq}(N)$, and for (III) and (IV) with N—H distances restrained to 0.88 and 0.86 Å, respectively. The hydroxyl groups of (I) and (II) were idealized with O—H distances of 0.84 Å and refined as rigid bodies, with $U_{iso}(H) = 1.2U_{eq}(O)$.

Data collection: *COLLECT* (Nonius, 1998) for (I), (II) and (III); *SMART* (Bruker, 1998) for (IV). Cell refinement: *DENZO* (Otwinowski & Minor, 1997) and *COLLECT* for (I), (II) and (III); *SAINT* (Bruker, 2000) for (IV). Data reduction: *DENZO* and *COLLECT* for (I), (II) and (III); *SAINT* for (IV). For all compounds, program(s) used to solve structure: *SHELXS97* (Sheldrick, 1997); programs(s) used to refine structure: *SHELXL97* (Sheldrick, 1997); molecular graphics: *ORTEP-3 for Windows* (Farrugia, 1997); software used to prepare material for publication: *SHELXL97* and *PLATON* (Spek, 2003).

The use of the EPSRC X-ray crystallographic service at Southampton and the valuable assistance of the staff there, particularly in indexing the intensity data from the twinned crystal of (I), are gratefully acknowledged.

Supplementary data for this paper are available from the IUCr electronic archives (Reference: GD1371). Services for accessing these data are described at the back of the journal.

References

Bernstein, J., Davis, R. E., Shimoni, L. & Chang, N.-L. (1995). *Angew. Chem. Int. Ed. Engl.* **34**, 1555–1573.
Blessing, R. H. (1995). *Acta Cryst.* A**51**, 33–37.
Blessing, R. H. (1997). *J. Appl. Cryst.* **30**, 421–426.
Boechat, N. & Pinto, A. de C. (2000). US Patent No. 6 034 266.
Bruker (1998). *SMART*. Version 5.054. Bruker AXS Inc., Madison, Wisconsin, USA.
Bruker (2000). *SAINT*. Version 6.02a. Bruker AXS Inc., Madison, Wisconsin, USA.
Farrugia, L. J. (1997). *J. Appl. Cryst.* **30**, 565.
Flack, H. D. (1983). *Acta Cryst.* A**39**, 876–881.
Nonius (1998). *COLLECT*. Nonius BV, Delft, The Netherlands.
Otwinowski, Z. & Minor, W. (1997). *Methods in Enzymology*, Vol. 276, *Macromolecular Crystallography*, Part A, edited by C. W. Carter Jr & R. M. Sweet, pp. 307–326. New York: Academic Press.
Sheldrick, G. M. (1997). *SHELXS97* and *SHELXL97*. University of Göttingen, Germany.
Sheldrick, G. M. (2000). *SADABS*. Version 2.03. Bruker AXS Inc., Madison, Wisconsin, USA.
Sheldrick, G. M. (2003). *SADABS*. Version 2.10. Bruker AXS Inc., Madison, Wisconsin, USA.
Spek, A. L. (2003). *J. Appl. Cryst.* **36**, 7–13.